

Roads towards fault-tolerant universal quantum computation

Earl T. Campbell

Department of Physics and Astronomy, University of Sheffield, Sheffield, UK

Barbara M. Terhal and Christophe Vuillot

JARA Institute for Quantum Information, RWTH Aachen University, 52056 Aachen, Germany

(Dated: November 13, 2018)

Current experiments are taking the first steps toward noise-resilient logical qubits. Crucially, a quantum computer must not merely store information, but also process it. A fault-tolerant computational procedure ensures that errors do not multiply and spread. This review compares the leading proposals for promoting a quantum memory to a quantum processor. We compare magic state distillation, color code techniques and other alternative ideas, paying attention to relative resource demands. We discuss the several no-go results which hold for low-dimensional topological codes and outline the potential rewards of using high-dimensional quantum (LDPC) codes in modular architectures.

I. INTRODUCTION

The next decade will likely herald controllable quantum systems with 30 or more physical qubits on various quantum technology platforms, such as ion-traps^{1,2} or superconducting qubits³. It may be difficult to simulate such partially-coherent, dynamically-driven, many-body systems on a classical computer, since the elementary two-qubit entangling gate time can be as much as a 1000 times faster than the single-qubit dephasing and relaxation times (T_2 and T_1). On the other hand, a system in which one out of a 1000 components fails is unlikely to perform well in executing large quantum algorithms designed for fault-free components. We must either figure out what computational tasks a noisy many-body quantum system can perform well or we use partially-coherent qubits as the elementary constituents of more robust logical qubits through quantum error correction. The choice of quantum error correcting architecture determines all operations at the physical hardware level. It constrains the compilation from quantum software and quantum algorithms to actions on elementary qubits in hardware. For superconducting qubits, efforts to build a first logical qubit of the surface code are underway at places such as IBM Research^{4,5}, UCSB in partnership with Google⁶ and the TU Delft⁷.

Quantum error correction works by making quantum information highly redundant so that errors affecting a few degrees of freedom become correctable⁸. One can formulate some rough desiderata of a quantum error correcting architecture which aim at minimizing experimental complexity: (1) the architecture has a high noise threshold, providing logical qubits that have a lower logical error probability per logical gate than their physical constituent qubits, (2) it allows for the implementation of a universal⁹ set of logical gates, and (3) it achieves these goals with low spatial (number of physical qubits per logical qubit) and temporal overhead (time duration of logical gate versus physical gate). In addition, (4) it should be possible to process error information sufficiently fast, keeping up with the advancing quantum computation. A

last desired property (5) may be that the code is a LDPC (low-density parity check) code: each parity check¹⁰ involves at most k qubits (parity check weight k) and each qubit participates in at most l parity checks (qubit degree l) where both l and k are small constants. Strongly preferred for solid-state qubits is a code for which the parity checks act on neighboring qubits in a 2D or 3D array.

An important universal gate set is the Clifford+ T set. The subset of Hadamard H , CNOT and $S = \text{diag}(1, e^{i\pi/2})$ are Clifford gates. A quantum circuit comprising only Clifford gates is not universal and confers no quantum computational advantage as it can be classically simulated by the Gottesman-Knill theorem^{11,12}. When single-qubit gates come about through resonant driving fields, rotating the qubit vector around its Bloch sphere, a $T = \text{diag}(1, e^{i\pi/4})$ gate is similar in complexity to an S or H gate. For a logical qubit, say, the one encoded by Steane's 7-qubit code (Box 1), the logical Hadamard is implemented by applying a Hadamard gate on each of the seven physical qubits. This is advantageous since it takes the same time as an elementary Hadamard gate and the transversal¹³ character of the logical gate ensures that errors do not spread between qubits of the code. The S gate and the CNOT gate are similarly transversal for the Steane code, but the T gate is not. Certainly *some* sequence of single and two-qubit gates can be designed to enact a logical T gate. While this is true, the presence of two-qubit gates in such a T gate construction will entirely negate the benefits of using a logical qubit. A sequence of two-qubit gates can spread correctable single-qubit errors to uncorrectable multi-qubit errors, making the logical qubit error probability higher than the error probability of a single constituent qubit.

Transversal logical gates are the easiest example of fault-tolerant logical gates, meaning logical gates which do not convert correctable errors into uncorrectable ones. Transversal gates are optimal in both spatial and temporal overhead. However, it was proved^{14,15} that no non-trivial code allows for the transversal implementation of all gates needed for universality, demonstrating the need

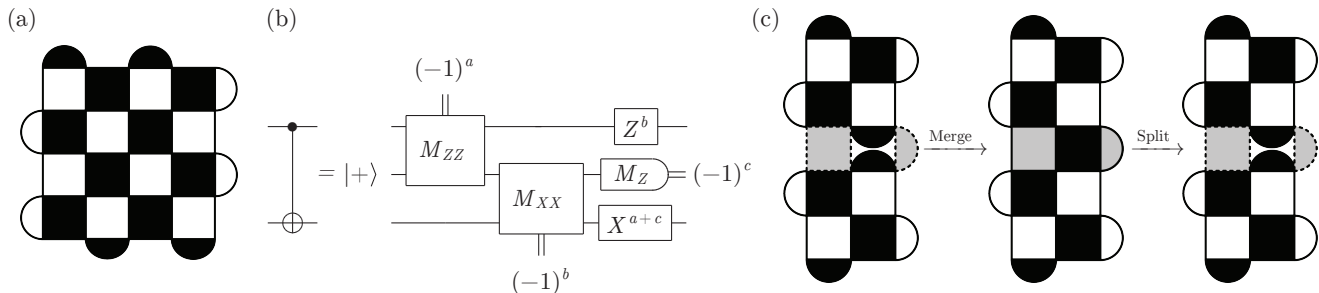


FIG. 1. (a) One logical qubit is encoded in a surface code sheet consisting of d^2 physical qubits at the vertices of the lattice ($d = 5$ in the Figure). Black faces represent X -parity checks and white faces represent Z -parity checks on the qubits. (b) A CNOT circuit is equivalent to performing non-destructive XX and ZZ measurements for the control and target qubits with an ancillary qubit. Lattice code surgery provides a method for non-destructively measuring a logical ZZ or XX between two encoded qubits. (c) Lattice code surgery between two surface code sheets which realizes a logical ZZ measurement. By measuring and merging the parity checks between two surface code sheets, we merge the two sheets into one. At the same time one learns the value of the logical ZZ as it equals the product of the newly measured grey faces. The two sheets can then be split again for further operations.

for other constructions.

A promising architecture uses the surface code, which was first put forward as a topological quantum memory¹⁸. It has a high noise threshold $p_c \approx 0.6 - 1\%$ ¹⁹⁻²¹ and requires only a 2D qubit connectivity with qubit degree 4. One logical qubit comprises d^2 physical qubits (plus $d^2 - 1$ ancilla qubits for parity check measurements) for a code distance d , see Fig. 1. Besides this encoding, there are at least two other ways of defining logical qubits in the surface code. A logical qubit can comprise two holes in an extended surface code sheet²² or a logical qubit could be represented by two pairs of lattice defects or twists^{23,24}. The logical error probability per round of parity check measurements P_L is determined by the distance, i.e. $P_L \propto (p/p_c)^{d/2}$. Numerical studies²¹ estimate that, assuming a depolarizing error probability $p < 10^{-3}$ per elementary gate, a logical qubit will consist of more than 10^4 physical qubits in order for $P_L < 10^{-15}$.

How does the surface code architecture handle the fault-tolerant implementation of gates? This is partially achieved by code deformation, which is a versatile technique used in fault-tolerantly executing the logical gates: The code is altered by changing which parity check measurements are done where. A logical CNOT can be obtained with the encoding in Fig. 1 through a deformation technique called lattice code surgery²⁵, see Fig. 1b and 1c. The encoding of Fig. 1 can also be deformed to a twist defect encoding where the four corners of the lattice correspond to four defects²⁶. Braiding of the four twist defects through the bulk of the lattice then generates the single-qubit S and Hadamard gate²⁶. Hence all Clifford gates could be done in situ on 2D surface code sheets. Another common approach to logical S gates is shown in Fig. 2b and uses state injection of a $|Y\rangle \propto |0\rangle + i|1\rangle$ state, which is an inexpensive resource as it may be used many times^{27,28}.

II. TOWARDS UNIVERSALITY

A. First Ideas

The necessity of finding effective means to implement a universal set of gates was realized from the earliest beginnings of the field. One useful tool is the simple circuit, shown in Fig. 2a, where we replace executing the T gate by preparing the ancilla state $|A\rangle = TH|0\rangle$, called a T magic state. The circuit can be executed at the logical level where one encodes qubit and ancilla in a base code. Peter Shor provided the first construction²⁹ for fault-tolerantly preparing a Toffoli magic state. A similar construction^{16,30} was proposed for fault-tolerantly preparing a T magic state. In these constructions one uses the fact that the logical magic state is an eigenstate of a logical Clifford gate which is transversal for the base code. Ancillary cat states are used to fault-tolerantly project onto this eigenstate, see Fig. 2c, but the approach does not scale favourably for topological codes.

B. Magic State Distillation

The mindset of Magic State Distillation (MSD) is to accept a preparation procedure providing noisy magic states, and then proceed by filtering many noisy magic states into fewer, yet better quality states. Efficient protocols for magic state distillation are designed, almost exclusively, using an error correction code with a transversal non-Clifford gate, typically the T gate. We call this code the distillation code. The $[[15, 1, 3]]$ quantum Reed-Muller code was shown¹⁶ to have a transversal T , and using this code for magic state distillation was proposed by Bravyi and Kitaev³¹. The $[[15, 1, 3]]$ code is now also recognized as the smallest member of a 3D color code family, see Fig. 4. All MSD protocols work at the logical

Box 1 | Steane's Code

Andrew Steane's 7-qubit code $[[7,1,3]]$ is the smallest example of a 2D color code encoding a single logical qubit $k = 1$. The code is defined as the +1 eigenspace of the 3 sets of commuting X -parity checks S_X^r, S_X^g, S_X^b and Z -parity checks S_Z^r, S_Z^g, S_Z^b , acting on the 7 qubits located at the vertices. Quantum error correction proceeds by nondestructively measuring these parity checks using ancilla qubits. The X -operator of the logical qubit can be chosen as $\Pi_{i=1}^7 X_i$ and the Z -operator is $\Pi_{i=1}^7 Z_i$, both of which can be reduced to products of 3 Pauli operators (parity check weight 3) by multiplication with check operators. The code distance is thus 3. The symmetry between X and Z -checks ensures that Hadamard and S gates can be implemented transversally. Seven CNOT gates between two blocks of Steane code realize the logical CNOT as can be verified from its action on the logical operators and the stabilizer group generated by the parity check operators. It was shown¹⁶ that one can implement a fault-tolerant controlled- S gate between two Steane blocks by applying 7 rounds, each with 7 block-wise Controlled- S gates, each round followed by X error correction. This makes for a fault-tolerant universal set of gates. The Steane code has been implemented in ion-trap qubits¹⁷.

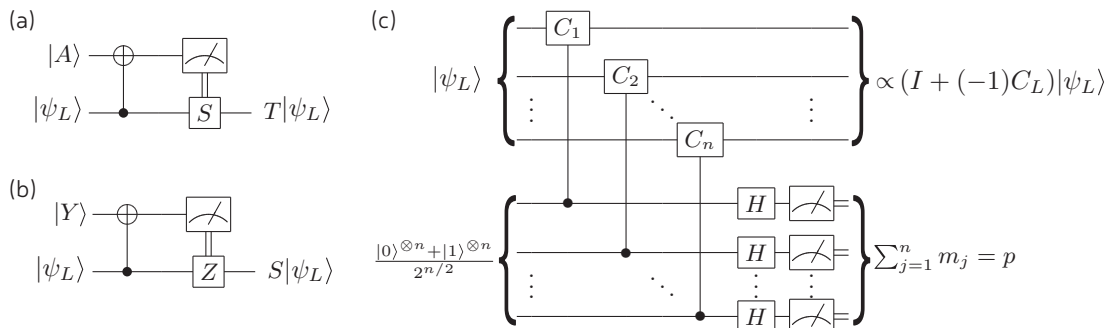
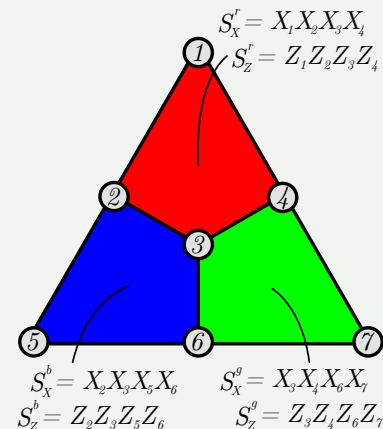


FIG. 2. (a) Implementation of a T gate via preparing the magic ancilla $|A\rangle = TH|0\rangle$. (b) Implementation of a S gate via preparing the magic ancilla $|Y\rangle = SH|0\rangle$. (c) Fault-tolerant implementation of the projection of a code state onto an eigenstate of a transversal logical Clifford gate $C_L = \prod_{j=1}^n C_j$ assuming that the Clifford gate C has ± 1 eigenvalues. To prepare a T magic state one takes $C = TXT^\dagger \propto SX$, using a transversal logical S gate for the base code. Since a single error can flip the outcome p , the circuit has to be repeated and a majority vote over the outcomes taken.

level of an underlying base code and so assume reliable Clifford operations. In Fig. 3 we outline one variant of MSD.

One figure of merit is the number of noisy magic states consumed per single T gate. Advances in distillation codes have improved the asymptotic efficiency by this metric (see Box 2). However, the number of physical qubits involved (space cost) and protocol duration (time cost) are more realistic metrics, although they depend on the choice of base code. When optimizing full space-time costs, an important trick is to increase the base code distance with successive distillation rounds (see step 5 of Fig. 3). Using this trick in conjunction with the surface code, resource overheads become dominated by the surface code cost in the final distillation round^{21,22,32,33}. This results in a space-time cost for the T gate that is only a constant multiple of a surface code overhead, namely a $O(d^2)$ spatial cost and a $O(d)$ temporal cost.

More precisely, the space-time cost of a T gate realized in a distance- d surface code is $C_T d^3$ with $C_T \approx 160 - 310$ when employing Bravyi-Haah codes^{21,32,33}. For Clifford gates the overhead per logical gate is also $O(d^3)$ but the constant prefactor is of order of unity. Using even higher yield MSD protocols (see Box 2) may reduce the C_T factor further, with the Bravyi-Haah codes already shown³² to have three times lower space-time costs than $[[15,1,3]]$.

Obtaining a fault-tolerant logical T gate is only a partial goal as Clifford+ T gates are then used to synthesize other logical gates needed in quantum algorithms³⁴⁻³⁷. A more efficient solution can be to directly distill magic states providing the most frequently required logic gates. Magic state distillation has been shown for smaller angle Z rotations³⁸⁻⁴⁰, the Toffoli gate^{41,42}, and a general class of multi-qubit circuits⁴³.

Given that magic state distillation takes up space and time, it requires an allocation of resources and commu-

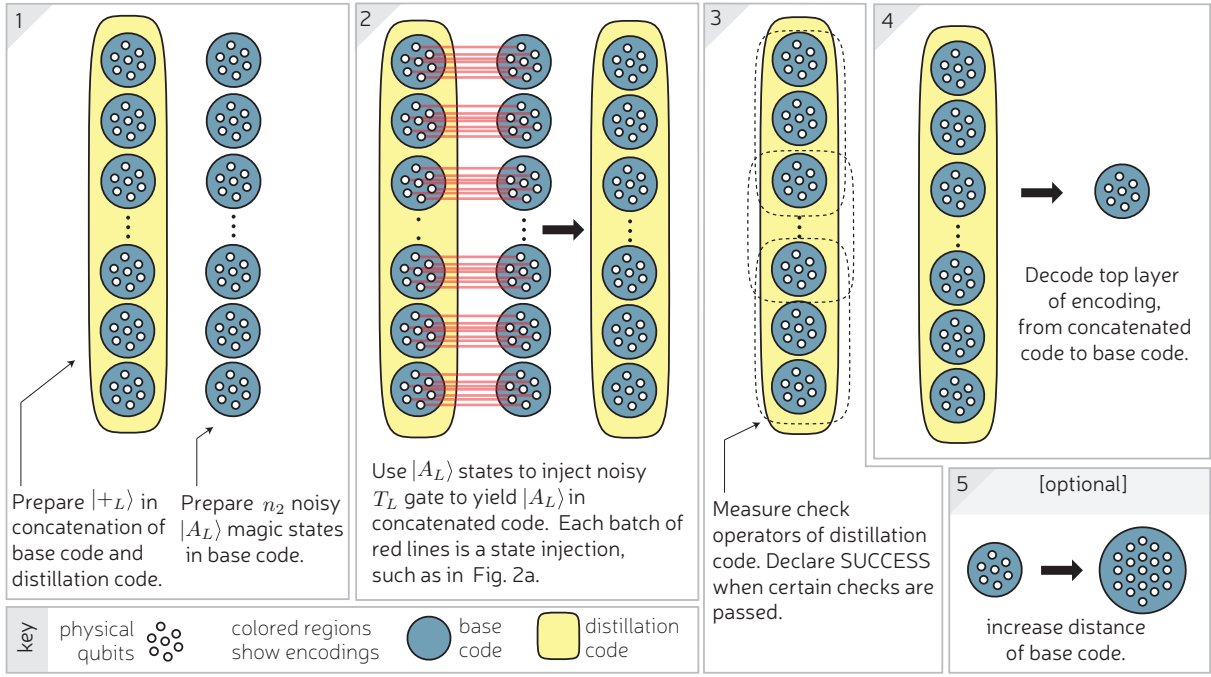


FIG. 3. Sketch of magic state distillation using a $[[n_2, 1, d_2]]$ distillation code with a transversal T gate, while Clifford operations are protected by a $[[n_1, 1, d_1]]$ base code. Given fewer than d_2 errors in the noisy magic states, they are detected in step 3. This implies that the logical error probability is suppressed from ϵ to $O(\epsilon^{d_2})$. Iterating r times, the error probability reduces to $O(\epsilon^{d_2^r})$.

nication infrastructure (in the form of logical roads) to these resources inside the 2D surface code architecture. Clifford gates in such an architecture could be done in situ on a ‘Clifford substrate’ of 2D surface code sheets. Throughout this 2D array of sheets, areas are reserved for magic state distillation factories for non-Clifford gates. The optimal spatial density of these factories depends on the typical quantum algorithmic use (frequency, parallelism) of non-Clifford gates. Clearly, any design of such a quantum computer will require a huge effort in integrated quantum circuit design and optimization, a quantum analog to VLSI design. This effort has barely gotten underway⁴⁴.

C. Color Codes

The $[[7,1,3]]$ and $[[15,1,3]]$ codes are the smallest members of a family of 2D and 3D, respectively, color codes^{55–57}. Examples are given in Fig. 4. These color codes retain the transversality properties of their respective smallest instances. Therefore, the 2D color codes have transversal Clifford gates^{58–60}. The 3D color codes can have a transversal non-Clifford gate^{53,56}, such as a T gate in the tetrahedral 3D color code. Lattice code surgery⁶¹ can again be used to locally perform CNOT gates. Color codes can also be extended to higher dimensions (see Box 3), with transversality properties related to the dimensionality.

The 3D color code does not have the symmetry between X - and Z -checks, and so lacks a transversal Hadamard gate. Ideas to get around this caused a surge of interest in 3D color codes. One idea is that of switching between different (3D color) codes via the important concept of gauge fixing^{60,62}. Using gauge fixing it is possible to use the transversal T gate of the 3D color code while only doing error correction and the Hadamard gate with the 3D gauge color code⁶³. The advantage of using the 3D gauge color code over the 3D color code, see Table I, are the lower parity check weights and the feature of single-shot error correction of the 3D gauge color code (see Sec. III C). A CNOT gate realized via lattice code surgery allows for the injection of the T gate from a 3D gauge color code into a 2D color code^{64,65}. One can imagine a 2D color code architecture augmented with 3D gauge color code T -stations where logical qubits can undergo a T gate, similar as a 2D surface code with 2D non-Clifford processing occurring at dedicated locations.

We summarize some of the known thresholds and properties of codes in Table I. Note that the 3D color and gauge color codes have a cubic spatial overhead $O(d^3)$ for a given distance d while this overhead is $O(d^2)$ for 2D codes. The complexity of decoding 3D color and 3D and 4D surface codes poses new challenges and is not fully understood while good algorithms exist for surface code decoding. The best thresholds for 2D color codes are lower than those of the surface code, possibly due to the fact that parity checks have higher weight.

Box 2 | High yield MSD

The yield is the number of distilled magic states, on average, per input noisy magic state. Using an $[[n_2, k_2, d_2]]$ distillation code for enough rounds to achieve some target ϵ_{out} has an asymptotic yield $1/O(\log(\epsilon_{\text{out}}^{-1})^\gamma)$ where $\gamma = \log_{d_2}(n_2/k_2)$. Therefore, lower γ values indicates more efficient distillation protocols. More sophisticated protocols (see table) can reduce the scaling factor γ , with $\gamma = 1$ conjectured⁴⁶ to be optimal.

Protocol	$[[n, k, d]]$	$\lim_{n \rightarrow \infty} \gamma$
Reed-Muller	$[[15, 1, 3]]$	2.464
Meier-Eastin-Knill ⁴⁵	$[[10, 2, 2]]$	2.322
Bravyi-Haah ⁴⁶	$[[3k + 8, k, 2]]$	1.585
Jones 2 nd level ⁴⁷	$[[5k + O(1), k, 4]]$	1.160
Jones r^{th} level ⁴⁷	$[[(2^r + 1)k + O(1), k, 2^r]]$	1

Code	Qubit Degree	Parity Check Weight	Threshold (Phen. Model)	Threshold (Circuit Model)	Single-Shot	Logic
2D Surface	4	4	2.9% ⁴⁸	0.6% ¹⁹ -1% ^{20,21}	No	Clifford
2D 6.6.6 Color	6	6	2.8% ^{49,50}	0.3% ^{49,50}	No	Clifford
3D Gauge Color	12	6	0.31% ⁵¹	Unknown	Yes	Clifford
3D Color	10	24	Unknown	Unknown	No	Transversal T
4D Surface	8	6	1.59% ⁵²	Unknown	Yes	†

TABLE I. Parity check weight is given for the bulk of the code lattice. The threshold depends on noise model: The phenomenological model assigns probability p equally to X & Z errors and an error in the parity check measurements; The circuit model applies depolarizing noise with probability p to every elementary component in the circuit implementing the parity checks. The phenomenological threshold is always higher than circuit model threshold, especially for codes with high parity check weight. †It has been shown⁵³ that one can perform a fault-tolerant non-Clifford 4-qubit-controlled- Z using a constant depth circuit.

However, 2D color code decoding is also more computationally complex than surface code decoding⁶⁶. The best threshold numbers for circuit-based noise in which each gate undergoes depolarizing noise with probability p are 0.3%^{49,50} for a triangular color code and 0.41% for a half-color or $[[4, 2, 2]]$ -concatenated toric code⁶⁷ (compare with 0.6 – 1% for the surface code).

D. Alternative Code Constructions

An alternative to topological error correction is concatenated coding in which the physical qubits in a code block are repeatedly replaced by logical qubits. Extensive work⁶⁸ has been performed on comparing the overheads and noise thresholds of various schemes. For a (concatenated) $[[23, 1, 7]]$ Golay code (with a transversal Clifford set) it has been shown that the asymptotic noise threshold is at least 0.13%⁶⁹ (compare with the numerical value 0.6 – 1.0% of the asymptotic surface code). Any concatenated scheme with easy Clifford gates could be combined with magic state distillation. The performance comparison with the surface code would largely rely on how much spatial overhead one pays for a logical Clifford gate.

Another concatenation idea is to combine the transversality of different gates in two different codes⁷⁰ and get rid of magic state distillation. For example, one can choose $[[7, 1, 3]]$ as a top code, i.e. replacing each physical qubit by 7, and then take $[[15, 1, 3]]$ as bottom code, replacing each of the 7 qubits again by a block of 15. The resulting code is $[[105, 1, 9]]$. Due to the non-transversality of the Hadamard at the bottom level and the non-transversality

of the T gate at the top level, the total logical error probability of these gates will suffer, but single-qubit errors can still be corrected in this construction. The asymptotic noise threshold of this construction was lower-bounded by 0.28%⁷¹.

In Box 1 it was stated that the Steane code has a *pieceable fault-tolerant*⁷² Controlled- S gate. This means that we can break down the execution of the gate in rounds or pieces, each round containing X error-correction to maintain fault-tolerance, but holding off on Z error correction until the entire gate is done. This idea does not easily scale to topological codes, but it could be analyzed for concatenated codes. It obviates the need for magic state distillation, but trades this, mostly likely, with a poorer asymptotic noise threshold.

Any scheme based on the concatenation of small codes can be converted to a coding scheme that is local in 1D or 2D at the cost of some additional overhead for gates which move qubits. If a large 3D color code is implemented in pure 2D hardware, it requires non-planar connections whose length grows with the size of the color code. Recent work^{73–75} has shown how to systematically construct codes that have a transversal T gate and convert these codes to so-called doubled color or 2D gauge color codes. However, by making all connections local on a 2D lattice the resulting 2D codes are non-topological. This means that the code performance is maximal for a certain code size and declines for larger code sizes. The performance of doubled color or 2D gauge color codes in producing a low-noise logical T ancilla (which can then be transferred to the 2D Clifford substrate) has not yet been compared with MSD or the usage of 3D T stations.

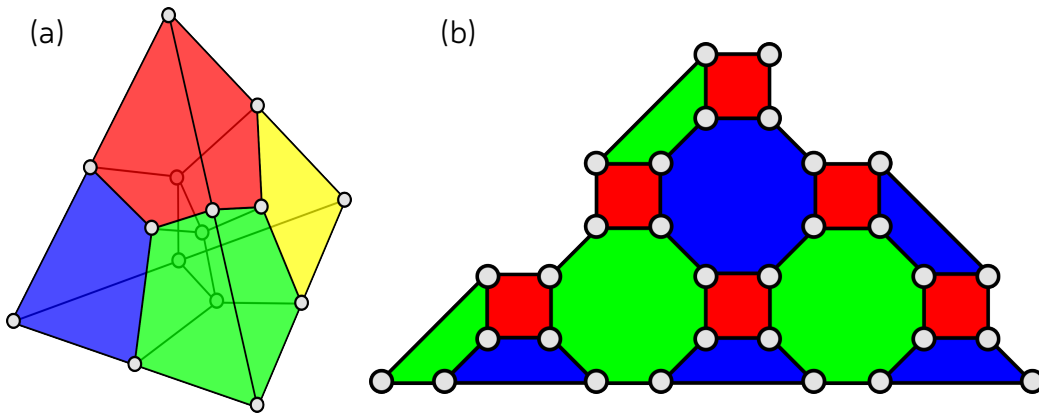


FIG. 4. (a) Smallest example $[[15, 1, 3]]$ of a tetrahedral 3D color code with qubits on the vertices. Each colored cell corresponds to a weight-8 X -check and each face corresponds to a weight-4 Z -check. A logical Z is any weight-3 Z -string along an edge of the entire tetrahedron. The logical X is any weight-7 X -face of the entire tetrahedron. A logical T^\dagger is implemented by applying a T gate on every qubit. The online Supplementary Information⁵⁴ has a movie of a larger 3D color code. (b) A 2D triangular $[[31, 1, 7]]$ code, generalizing Steane’s code, based on a 4.8.8. lattice. The qubits are associated with vertices and each colored face corresponds to both an X and a Z -check. A logical X or Z is a X -string (resp. Z -string) running along any of the edges of the entire triangle.

Box 3 | Arbitrary dimension color codes

The general construction D -dimensional gauge or stabilizer color codes is based on a D -dimensional simplicial complex whose vertices are $D + 1$ -colorable (adjacent vertices have different colors). One associates qubits with D -simplices, X - and Z -parity checks with respectively x - and z -simplices, obeying $x + z \leq D - 2$. This inequality and the colorability property enforce the commutation of the checks, leading to a code family $\text{ColorCode}_D(x, z)$ ^{59,60}. A common boundary configuration for such codes is obtained by tiling the inside of a big D -simplex, respecting colorability but omitting elements of the bigger simplex as possible checks (see Suppl. Inf.⁵⁴ for the construction of a 3D code). Such color codes encode one logical qubit and we can call them simplicial color codes.

In 2D qubits are on triangles and the only choice is $x = z = 0$. This implies that a X - and a Z -parity check is associated with each vertex, leading directly a transversal H gate. The simplicial (or triangular) version also has a transversal S gate. The common representation of such codes, Fig. 4, is obtained by going to the dual lattice where qubits are associated with vertices and checks are associated with faces of the lattice.

For dimensions higher than 2D, it is possible to choose $x + z < D - 2$. In that case, the code space contains gauge qubits whose X - and Z -gauge checks are given respectively by $(D - 2 - z)$ - and $(D - 2 - x)$ -simplices. Remarkably, the gauge checks redundantly represent the stabilizer check information giving rise to single-shot error correction, discussed in III C. In 3D qubits are on tetrahedra and one has three choices for (x, z) . Choosing $(x, z) = (0, 0)$ gives a 3D gauge color code⁶⁰. This code has a X - and Z -stabilizer check for each vertex leading to a transversal Hadamard and gauge checks associated with edges. Another option is the 3D color family with $(x, z) = (0, 1)$ in which the X -checks are associated with vertices and the Z -checks with edges. The simplicial (or tetrahedral) version of this 3D color code has a transversal T ⁵⁵ and the smallest example $[[15, 1, 3]]$ is shown in Fig. 4a. The third option $(x, z) = (1, 0)$ is trivially (Clifford) equivalent to the $(x, z) = (0, 1)$ codes.

E. Comparison of Resource Overheads

The combination of MSD with the surface code is currently considered a competitive scheme since it combines a high-noise threshold, a 2D architecture and a T gate that is a few hundred times as costly as Clifford gates in terms of its space-time overhead. Replacing MSD by 3D T -gate stations and/or the surface code substrate by a color code substrate is an alternative whose appeal depends on the physical error probability versus the 2D and 3D color code thresholds. The use of the 3D gauge color

code for a T gate requires $O(d^3)$ qubits, but single-shot error correction makes the space-time cost again $O(d^3)$ ⁶³.

An analysis⁷¹ of the concatenation scheme discussed in Sec. IID shows that the spatial overhead is still not favorable as compared to using surface codes with MSD. This analysis includes the consideration of a smaller, more efficient, 49-qubit code⁷⁶. To get to the target error probability $P_L < 10^{-15}$ starting with a physical error probability of $O(10^{-5})$ it is estimated that the concatenated scheme uses at least 10^7 physical qubit for a logical qubit (versus 10^4 for surface codes with MSD).

III. THE BLESSING OF DIMENSIONALITY?

A. Transversality and Dimensionality

A deep connection between transversality and dimensionality of a topological stabilizer code was proved by Bravyi and Koenig⁷⁷. Their theorem says that for D -dimensional topological stabilizer codes, the only logical gates that one can implement via a transversal or constant depth circuit are in the so-called m^{th} level of the Clifford hierarchy \mathcal{C}_m . Here \mathcal{C}_1 is the group of n -qubit Pauli operators, \mathcal{C}_2 is the Clifford group, \mathcal{C}_3 contains gates such as T and Toffoli and the m^{th} level includes a small rotation gate such as $\text{diag}(1, \exp(\frac{2\pi i}{2^m}))$. While the gate set Clifford+ T is universal, it can be shown that using gates in higher levels of the Clifford hierarchy reduces the time overhead associated with gate synthesis. The gates that one can realize with D -dimensional color and surface codes saturate the Bravyi-Koenig theorem^{53,59,60}. This theorem does not prove that there are no good 2D alternatives to magic state distillation. It does suggest that any alternative might come at the price of a lower threshold for universal quantum logic as it requires a non-trivial fault-tolerant gate construction.

B. Tradeoff Bounds

For the design of a storage medium, a quantum hard-drive, one can drop the universal gate set desideratum (2) as long as quantum information can be read and written to storage. Ideally, the storage code is a $[[n, k, d]]$ code with high rate k/n and high distance d scaling as some function of n . It was shown⁷⁸ that 2D Euclidean topological stabilizer codes are constrained by $kd^2 \leq cn$ for some constant c : the surface code clearly saturates this bound. The adjective Euclidean means that the qubits can be placed on a 2D regular grid with each qubit connecting to $O(1)$ neighbors. Consequently, the rate of these codes vanishes with increasing distance, leading to a substantial overhead as a storage code. Hyperbolic surface codes⁷⁹ are only bound by $kd^2 \leq c(\log k)^2 n^{80}$. There is a simple hyperbolic surface code in which qubits are placed on the edges of square tiles and five tiles meet at a vertex. Such $\{5, 4\}$ -hyperbolic surface codes have an asymptotic rate $\frac{k}{n} = \frac{1}{10}$ and logarithmically growing distance⁷⁹.

C. Single-shot Error Correction

2D topological codes have an intrinsic temporal overhead in executing code deformation in a fault-tolerant manner, making gates that rely on this technique take $O(d)$ time. The reason is that in code deformation new parity check measurements are repeated $O(d)$ times in order for this record to be sufficiently reliable. The absence of redundancy in the parity check measurement record is an immediate consequence of the lack of self-correction

of 2D topological stabilizer codes⁸¹. A 4D hypercubic lattice version of the surface code¹⁸ allows for *single-shot* error correction instead. Due to redundancy in the parity check data in this code, it is possible to repair the data for measurement errors after a single round of measurement. Codes which have such single-shot error correction then have potentially higher noise thresholds and faster logical gates. Interestingly, Bombin showed that single-shot error correction is possible for 3D gauge color codes⁶³. For such code the value of the stabilizer parity checks is acquired through measuring non-commuting lower-weight gauge qubit checks whose products determine the stabilizer parity checks. Curiously, in the 3D gauge color code, the gauge qubit checks hold redundant information, which allows one to construct a robust record for the stabilizer parity checks in $O(1)$ time. The result shows the power of using subsystem codes with gauge degrees of freedom since we do not expect to have single-shot error correction for 3D stabilizer codes.

IV. OUTLOOK

We have discussed several ideas for adding universal computing power to a quantum device. Presently, using surface codes with magic state distillation is the most practical solution. We have seen that there is a wealth of fascinating alternatives, but so far they have yet to demonstrate a comparably high threshold or significant improvements in resource scaling. A interesting direction is to move away from the constraints of low dimensional topological codes.

More general LDPC codes could be considered, for example the 4D surface code in Table I. Homological quantum (LDPC) codes can in principle be constructed from tilings of any D -dimensional manifold. Generalizations of classical LDPC codes based on expander graphs to quantum codes are also known to exist^{82,83}.

Such approaches require hardware that supports long-range connectivity. Fortunately, various long-range experimental platforms such as ion-trap qubits or nuclear spins coupled to NV centers in diamond, do not necessarily conform to the paradigm of a 2D ‘sea’ of qubits. One may expect such architectures to work with modular components with photonic interconnects^{84,85}, which would allow for more flexible and long-range connectivity.

The advantage of using a higher-dimensional LDPC code or more general quantum LDPC code for computation or storage in a concrete coding architecture remains to be fully explored, in particular efficient decoding software needs to be developed. Independent of whether these codes can be used in a coding architecture, we expect that the study and development of quantum LDPC codes will lead to new insights into robust macroscopic quantum information processing.

V. ACKNOWLEDGEMENTS

BMT and CV acknowledge support through the EU via the ERC GRANT EQEC and ETC is supported by the EPSRC (EP/M024261/1).

-
- ¹ H. Haefner, C. Roos, and R. Blatt, *Physics Reports* **469**, 155 (2008).
- ² C. Ballance, T. Harty, N. Linke, M. Sepiol, and D. Lucas, *Phys. Rev. Lett.* **117**, 060504 (2016).
- ³ M. H. Devoret and R. J. Schoelkopf, *Science* **339**, 1169 (2013).
- ⁴ A. D. Córcoles, E. Magesan, S. J. Srinivasan, A. W. Cross, M. Steffen, J. M. Gambetta, and J. M. Chow, *Nature Communications* **6**, 6979 (2015).
- ⁵ J. M. Gambetta, J. M. Chow, and M. Steffen, *ArXiv e-prints* (2015), arXiv:1510.04375 [quant-ph].
- ⁶ J. Kelly, R. Barends, A. Fowler, A. Megrant, E. Jeffrey, T. White, D. Sank, J. Mutus, B. Campbell, Y. Chen, *et al.*, *Nature* **519**, 66 (2015).
- ⁷ D. Ristè, S. Poletto, M.-Z. Huang, A. Bruno, V. Vesterinen, O.-P. Saira, and L. Dicarlo, *Nature Communications* **6**, 6983 (2015).
- ⁸ B. Terhal, *Rev. Mod. Phys.* **87**, 307 (2015).
- ⁹ A discrete set of gates is universal if the gates in the set can be composed to make any desired unitary gate up to arbitrary precision.
- ¹⁰ Parity checks operators are operators that define the code space and return a +1 outcome when measured in the absence of errors.
- ¹¹ D. Gottesman, *Stabilizer Codes and Quantum Error Correction*, Ph.D. thesis, CalTech (1997), <http://arxiv.org/abs/quant-ph/9705052>.
- ¹² S. Aaronson and D. Gottesman, *Phys. Rev. A* **70**, 052328 (2004).
- ¹³ For a single block of code transversal logical gates are realized as a product of single-qubit unitary gates. Transversal logical gates between multiple blocks may use non-product unitary gates provided that these interactions are only between the different blocks.
- ¹⁴ X. Chen, H. Chung, A. W. Cross, B. Zeng, and I. L. Chuang, *Phys. Rev. A* **78**, 012353 (2008).
- ¹⁵ B. Eastin and E. Knill, *Phys. Rev. Lett.* **102**, 110502 (2009).
- ¹⁶ E. Knill, R. Laflamme, and W. Zurek, “Threshold accuracy for quantum computation,” (1998), quant-ph/9610011.
- ¹⁷ D. Nigg, M. Mueller, E. A. Martinez, P. Schindler, M. Hennrich, T. Monz, M. A. Martin-Delgado, and R. Blatt, *Science* **345**, 302 (2014).
- ¹⁸ E. Dennis, A. Kitaev, A. Landahl, and J. Preskill, *J. Math. Phys.* **43**, 4452 (2002).
- ¹⁹ R. Raussendorf and J. Harrington, *Phys. Rev. Lett.* **98**, 190504 (2007).
- ²⁰ A. G. Fowler, A. M. Stephens, and P. Groszkowski, *Phys. Rev. A* **80**, 052312 (2009).
- ²¹ A. Fowler, M. Mariantoni, J. Martinis, and A. N. Cleland, *Phys. Rev. A* **86**, 032324 (2012).
- ²² R. Raussendorf, J. Harrington, and K. Goyal, *New J. Phys.* **9**, 199 (2007).
- ²³ H. Bombín, *Phys. Rev. Lett.* **105**, 030403 (2010).
- ²⁴ M. B. Hastings and A. Geller, *ArXiv e-prints* (2014), arXiv:1408.3379 [quant-ph].
- ²⁵ C. Horsman, A. G. Fowler, S. Devitt, and R. Van Meter, *New Journal of Physics* **14**, 123011 (2012).
- ²⁶ B. J. Brown, K. Laubscher, M. S. Kesselring, and J. R. Wootton, *ArXiv e-prints* (2016), arXiv:1609.04673 [quant-ph].
- ²⁷ P. Aliferis, *Level reduction and the quantum threshold theorem*, Ph.D. thesis, Caltech (2007).
- ²⁸ N. C. Jones, R. Van Meter, A. G. Fowler, P. L. McMahon, J. Kim, T. D. Ladd, and Y. Yamamoto, *Phys. Rev. X* **2**, 031007 (2012).
- ²⁹ P. W. Shor, in *37th Annual Symposium on Foundations of Computer Science, FOCS '96, Burlington, Vermont, USA, 14-16 October, 1996* (1996) pp. 56–65.
- ³⁰ E. Knill, R. Laflamme, and W. Zurek, *Science* **279**, 342 (1998).
- ³¹ S. Bravyi and A. Kitaev, *Phys. Rev. A* **71**, 022316 (2005).
- ³² A. G. Fowler, S. J. Devitt, and C. Jones, *Scientific reports* **3** (2013).
- ³³ J. O’Gorman and E. T. Campbell, *arXiv preprint arXiv:1605.07197* (2016).
- ³⁴ A. Y. Kitaev, A. Shen, and M. Vyalyi, *Classical and Quantum Computation. Vol. 47 of Graduate Studies in Mathematics.* (American Mathematical Society, Providence, RI, 2002).
- ³⁵ N. J. Ross and P. Selinger, *Quant. Inf. and Comp.* **16**, 901 (2016).
- ³⁶ A. Bocharov, M. Roetteler, and K. M. Svore, *Phys. Rev. A* **91**, 052317 (2015).
- ³⁷ M. Amy, D. Maslov, M. Mosca, and M. Roetteler, *IEEE Transactions on Computer-Aided Design of Integrated Circuits and Systems* **32**, 818 (2013).
- ³⁸ A. J. Landahl and C. Cesare, *arXiv preprint arXiv:1302.3240* (2013).
- ³⁹ G. Duclos-Cianci and D. Poulin, *Phys. Rev. A* **91**, 042315 (2015).
- ⁴⁰ E. T. Campbell and J. O’Gorman, *Quant. Sci. Tech.* **1**, 015007 (2016).
- ⁴¹ B. Eastin, *Phys. Rev. A* **87**, 032321 (2013).
- ⁴² C. Jones, *Phys. Rev. A* **87**, 022328 (2013).
- ⁴³ E. T. Campbell and M. Howard, *arXiv preprint arXiv:1606.01904* (2016).
- ⁴⁴ A. Paler, S. J. Devitt, and A. G. Fowler, *Scientific Reports* **6**, 30600 (2016), arXiv:1604.08621 [quant-ph].
- ⁴⁵ A. M. Meier, B. Eastin, and E. Knill, *Quant. Inf. and Comp.* **13**, 195 (2013).
- ⁴⁶ S. Bravyi and J. Haah, *Phys. Rev. A* **86**, 052329 (2012).
- ⁴⁷ C. Jones, *Phys. Rev. A* **87**, 042305 (2013a).
- ⁴⁸ C. Wang, J. Harrington, and J. Preskill, *Annals of Physics* **303**, 31 (2003).
- ⁴⁹ M. Beverland, A. Kubica, F. Brandao, J. Preskill, and K. Svore, To appear.

- ⁵⁰ M. Beverland, *Toward realizable quantum computers*, Ph.D. thesis, Caltech (2016).
- ⁵¹ B. J. Brown, N. H. Nickerson, and D. E. Browne, *Nature Communications* **7** (2016).
- ⁵² N. P. Breuckmann, K. Duivenvoorden, D. Michels, and B. M. Terhal, In press at QIC, ArXiv e-prints (2016), arXiv:1609.00510 [quant-ph].
- ⁵³ A. Kubica, B. Yoshida, and F. Pastawski, *New Journal of Physics* **17**, 083026 (2015).
- ⁵⁴ <https://youtu.be/erkeCxQ0-g4>.
- ⁵⁵ H. Bombín and M. A. Martin-Delgado, *Phys. Rev. Lett.* **97**, 180501 (2006).
- ⁵⁶ H. Bombín and M. A. Martin-Delgado, *Phys. Rev. Lett.* **98**, 160502 (2007).
- ⁵⁷ H. Bombín and M. Martin-Delgado, *Journal of mathematical physics* **48**, 052105 (2007).
- ⁵⁸ H. G. Katzgraber, H. Bombin, R. S. Andrist, and M. Martin-Delgado, *Physical Review A* **81**, 012319 (2010).
- ⁵⁹ A. Kubica and M. E. Beverland, *Phys. Rev. A* **91**, 032330 (2015).
- ⁶⁰ H. Bombín, *New Journal of Physics* **17**, 083002 (2015).
- ⁶¹ A. J. Landahl and C. Ryan-Anderson, “Quantum computing by color-code lattice surgery,” (2014), report SAND2014-15911J and arXiv:1407.5103.
- ⁶² A. Paetzniak and B. W. Reichardt, *Phys. Rev. Lett.* **111**, 090505 (2013).
- ⁶³ H. Bombín, *Phys. Rev. X* **5**, 031043 (2015).
- ⁶⁴ C. Vuillot and B. Terhal, To appear, 2016.
- ⁶⁵ H. Bombín, *New Journal of Physics* **18**, 043038 (2016).
- ⁶⁶ N. Delfosse, *Phys. Rev. A* **89**, 012317 (2014), arXiv:1308.6207 [quant-ph].
- ⁶⁷ B. Criger and B. Terhal, *Quant. Inf. and Comp.* **16**, 1261 (2016).
- ⁶⁸ A. W. Cross, D. P. DiVincenzo, and B. M. Terhal, *Quantum Info. and Comput.* **9**, 541 (2009).
- ⁶⁹ A. Paetzniak and B. W. Reichardt, *Quant. Inf. and Comp.* **12**, 1034 (2012).
- ⁷⁰ T. Jochym-O’Connor and R. Laflamme, *Phys. Rev. Lett.* **112**, 010505 (2014), arXiv:1309.3310 [quant-ph].
- ⁷¹ C. Chamberland, T. Jochym-O’Connor, and R. Laflamme, arXiv preprint arXiv:1609.07497 (2016).
- ⁷² T. J. Yoder, R. Takagi, and I. L. Chuang, *Phys. Rev. X* **6**, 031039 (2016).
- ⁷³ S. Bravyi and A. Cross, arXiv preprint arXiv:1509.03239 (2015).
- ⁷⁴ C. Jones, P. Brooks, and J. Harrington, *Phys. Rev. A* **93**, 052332 (2016), arXiv:1512.04193 [quant-ph].
- ⁷⁵ T. Jochym-O’Connor and S. D. Bartlett, *Phys. Rev. A* **93**, 022323 (2016).
- ⁷⁶ E. Nikahd, M. Sedighi, and M. S. Zamani, arXiv preprint arXiv:1605.07007 (2016).
- ⁷⁷ S. Bravyi and R. Koenig, *Phys. Rev. Lett.* **110**, 170503 (2013).
- ⁷⁸ S. Bravyi, D. Poulin, and B. M. Terhal, *Phys. Rev. Lett.* **104**, 050503 (2010).
- ⁷⁹ N. P. Breuckmann and B. M. Terhal, *IEEE Transactions on Information Theory* **62**, 3731 (2016).
- ⁸⁰ N. Delfosse, in *Information Theory Proceedings (ISIT), 2013 IEEE International Symposium on* (IEEE, 2013) pp. 917–921.
- ⁸¹ S. Bravyi and B. M. Terhal, *New Journal of Physics* **11**, 043029 (2009).
- ⁸² J.-P. Tillich and G. Zémor, in *Proceedings of the IEEE Symposium on Information Theory* (2009) pp. 799–803, <http://arxiv.org/abs/0903.0566>.
- ⁸³ M. H. Freedman and M. B. Hastings, *Quant. Inf. and Comp.* **14**, 144 (2014).
- ⁸⁴ C. Monroe, R. Raussendorf, A. Ruthven, K. Brown, P. Maunz, L.-M. Duan, and J. Kim, *Phys. Rev. A* **89**, 022317 (2014).
- ⁸⁵ N. H. Nickerson, J. F. Fitzsimons, and S. C. Benjamin, *Phys. Rev. X* **4**, 041041 (2014).